Hindawi Publishing Corporation
Mathematical Problems in Engineering
Volume 2012, Article ID 375080, 19 pages
doi:10.1155/2012/375080

Research Article

Control and Evaluation of Slow-Active Suspensions with Preview for a Full Car

Mohamed M. ElMadany

Mechanical Engineering Department, King Saud University, P.O. Box 800, Riyadh 11421, Saudi Arabia

Correspondence should be addressed to Mohamed M. ElMadany, mmadany@ksu.edu.sa

Received 31 July 2011; Accepted 24 October 2011

Academic Editor: Zhan Shu

An optimal control design method based on the use of the correlation between the front and rear wheel inputs (wheelbase preview) is introduced and then applied to the optimum design of a slow-active suspension system. The suspension consists of a limited bandwidth actuator in series with a passive spring, the combination being in parallel with a passive damper. A three-dimensional seven degrees of freedom car riding model subjected to four correlated random road inputs is considered. The performance potential of the limited bandwidth system with wheelbase preview in comparison with the nonpreview (uncorrelated inputs) case is investigated.

1. Introduction

Electronically controlled suspension systems have the potential to overcome limitations of passive systems and to reduce the need to compromise among a variety of operating conditions and among the generally conflicting goals of the suspension designs [1–7]. Such goals include providing good vibration isolation of the vehicle body (ride comfort), maintaining uninterrupted contact between the tire and the road (road-holding ability for ride handling), and stabilizing the vehicle body (ride safety). Researchers have studied active suspension systems using a number of different vehicle models, with optimum linear quadratic regulator control methods being widely used in the suspension design. Many investigators have utilized a two degree-of-freedom quarter car model with an active suspension [8–14]. These references have used full bandwidth suspension systems, which offer improvements in ride and handling qualities but may suffer from other problems such as complexity, high cost and power consumption and noise, vibration, and harshness problems [15, 16]. Consequently, such fully active systems have been unattractive commercially for production cars. However, it has been demonstrated that limited bandwidth active (slow-active) systems can offer significant improvements in the control of body

resonances, similar to full bandwidth systems [15, 16]. The slow-active systems may be envisioned as an actuator of limited bandwidth (around 3–5 Hz). This system has been realized commercially by gas springs and electrohydraulic elements [17, 18]. This type of system is of special interest for several reasons: (a) with an actuator bandwidth of 3 Hz, the actuators can be used to control roll in cornering and pitch in braking and accelerating such that poor handling need not to be a consequence of low wheel rates; (b) beyond the bandwidth of the actuator, the system is conventional; (c) relatively simple actuators which may be electrical or hydraulic will probably provide the necessary performance; (e) power consumption should be very modest.

In recent years, there has been a great interest in the use of preview of the road input in the design of active suspension systems, and very encouraging results in terms of improved performance have been obtained [19, 20]. Since the control law needs information on the road input some distance ahead of the front wheels, practical difficulties of measuring the road surface by a body-mounted road sensor are encountered.

Practically, however, as a vehicle travels straight on hard road surfaces, the rear wheel is subject to almost the same road input as the front wheel with only a time delay. The wheelbase preview information can be incorporated in the control law designs for active vehicle suspension systems, and further performance improvements are expected. The wheelbase preview control has been studied [21–23], and promising results have been obtained. The benefits come without additional costs for sensors. The aforementioned references have used preview information with unlimited bandwidth (fully active) systems. Pilbeam and Sharp [23] have used a half-car model to study the effect of the wheelbase preview on the performance capabilities of a slow-active suspension system. However, the derived preview-controlled system does not have zero steady-state axles to body deflection in response to external body forces due to changes in payload, aerodynamic forces, and forces from steering, braking, and traction.

The purpose of this study is to develop a full car model equipped with a slow-active suspension system and including integral control terms in order to control the pitch and roll modes of the car body. In addition, a control strategy especially designed to include wheelbase preview is presented in order to reduce the vibration of the car body and to evaluate the effects of this strategy on the performance of the limited bandwidth suspension systems. The process of synthesizing the control law is based on modifications of the control algorithm to account for tire road input correlation and penalizing the integral control terms in the performance index (cost function). This formulation provides needed flexibility in targeting body modes (pitch and roll) by control.

2. Car Ride Model

A schematic representation of the vehicle mathematical model is shown in Figure 1. It is seen to be a three-dimensional model with seven degrees of freedom. It considers bounce, pitch, and roll modes of the sprung mass and vertical (bounce) motions of the four unsprung masses. A slow-active suspension system is assumed to be incorporated between the sprung mass and the car axles at each corner as indicated in the figure. The slow-active system incorporates an actuator of limited bandwidth in series with a passive spring, the combination being in parallel with a passive damper. The actuator control bandwidth embraces the normal range of body resonant frequencies in bounce, pitch, and roll, but it does not extend as far as wheel-hop frequencies. This type of actuator is treated as

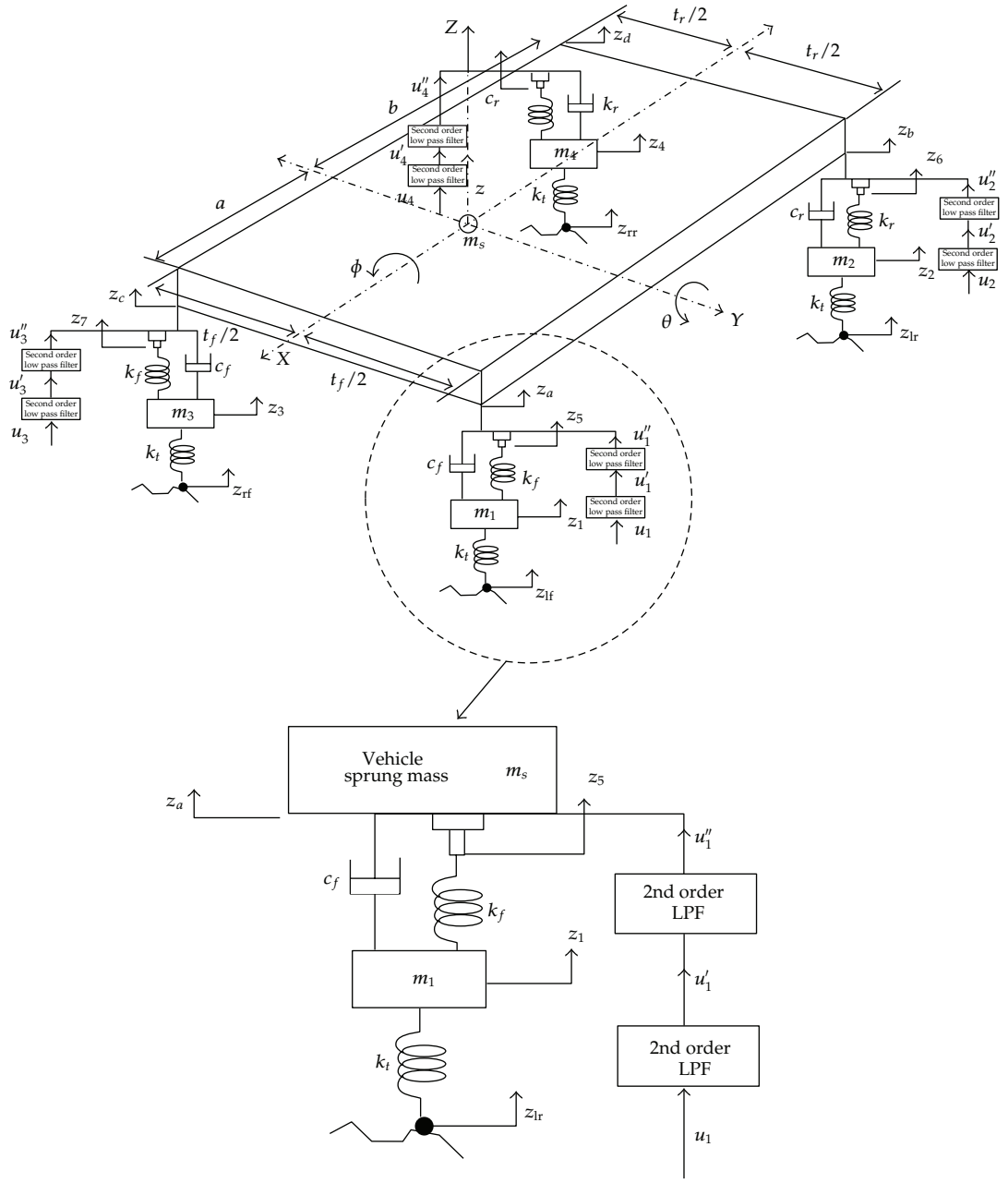

Figure 1: Slow-active suspension system.

a displacement producer. Its inner control loop would involve displacement feedback and the actuator demand signal will notionally be a desired displacement. The limited bandwidth nature of each actuator is represented in the vehicle model by including two similar second-order low-pass filters in series with a perfect actuator.

The equations governing the dynamic motion of the vehicle model equipped with slow-active suspension systems are briefly described below.

From Figure 1, the following equations may be derived: The equation of heave (vertical) motion of the sprung mass

$$m_s\ddot{z} = F_a + F_b + F_c + F_d. \tag{2.1}$$

the equation of roll motion of the sprung mass

$$I_x\ddot{\phi} = \frac{t_f F_a}{2} - \frac{t_f F_c}{2} + \frac{t_r F_b}{2} - \frac{t_r F_d}{2}, \tag{2.2}$$

the equation of pitch motion of the sprung mass

$$I_y\ddot{\theta} = -aF_a + bF_b - aF_c + bF_d, \tag{2.3}$$

the equations of vertical motion of the unsprung masses

$$\begin{aligned} m_1\ddot{z}_1 &= -F_a + k_t(z_{1\mathrm{f}} - z_1), \\ m_2\ddot{z}_2 &= -F_b + k_t(z_{1\mathrm{r}} - z_2), \\ m_3\ddot{z}_3 &= -F_c + k_t(z_{\mathrm{rf}} - z_3), \\ m_4\ddot{z}_4 &= -F_d + k_t(z_{\mathrm{rr}} - z_4). \end{aligned} \tag{2.4}$$

For the system in hand, the second-order low-pass filter (LPF) equations are:

$$\begin{aligned} \ddot{u}_i' + 2\varsigma\omega_c\dot{u}_i' + \omega_c^2 u_i' &= \omega_c^2 u_i, \quad i = 1,2,3,4, \\ \ddot{u}_i'' + 2\varsigma\omega_c\dot{u}_i'' + \omega_c^2 u_i'' &= \omega_c^2 u_i', \quad i = 1,2,3,4, \end{aligned} \tag{2.5}$$

where u_i' and u_i'' are the 2nd- and 4th-order filtered control demand signals, respectively, and

$$\begin{aligned} u_1'' &= z_a - z_5, & u_2'' &= z_b - z_6, \\ u_3'' &= z_c - z_7, & u_4'' &= z_d - z_8, \\ F_a &= k_f(z_1 - z_5) + c_f(\dot{z}_1 - \dot{z}_a), & F_b &= k_r(z_2 - z_6) + c_r(\dot{z}_2 - \dot{z}_b), \\ F_c &= k_f(z_3 - z_7) + c_f(\dot{z}_3 - \dot{z}_c), & F_d &= k_r(z_4 - z_8) + c_r(\dot{z}_4 - \dot{z}_d). \end{aligned} \tag{2.6}$$

With

$$\begin{aligned} z_a &= z + \frac{t_f}{2}\phi - a\theta, & z_b &= z + \frac{t_r}{2}\phi + b\theta, \\ z_c &= z - \frac{t_f}{2}\phi - a\theta, & z_d &= z - \frac{t_r}{2}\phi + b\theta. \end{aligned} \tag{2.7}$$

Introducing the following state, control input, and disturbance vectors:

$$\begin{aligned} x_p &= \left[\, \dot{\phi} \;\; \dot{\theta} \;\; \phi \;\; \theta \;\; z \;\; \dot{z} \;\; z_1 \;\; \dot{z}_1 \;\; z_2 \;\; \dot{z}_2 \;\; z_3 \;\; \dot{z}_3 \;\; z_4 \;\; \dot{z}_4 \;\; z_5 \;\; \dot{z}_5 \;\; z_6 \;\; \dot{z}_6 \;\; z_7 \;\; \dot{z}_7 \;\; z_8 \;\; \dot{z}_8 \right. \\ &\qquad \left. u_1' \;\; \dot{u}_1' \;\; u_2' \;\; \dot{u}_2' \;\; u_3' \;\; \dot{u}_3' \;\; u_4' \;\; \dot{u}_4' \,\right]^T, \\ u &= \left[u_1 \;\; u_2 \;\; u_3 \;\; u_4\right]^T, \qquad w = \left[z_{\mathrm{lf}} \;\; z_{\mathrm{lr}} \;\; z_{\mathrm{rf}} \;\; z_{\mathrm{rr}}\right]^T, \end{aligned} \tag{2.8}$$

the equations of motion can be expressed in the following state equation:

$$\dot{x}_p = A_p x_p + B_p u + D_p w, \tag{2.9}$$

where A_p, B_p, and D_p are matrices of dimensions $n \times n$, $n \times m$, and $n \times m$, where $n = 30$ and $m = 4$.

In order to control the body motion due to changes in payload forces, resulting from steering, braking, and traction, and aerodynamic forces, the system equations are augmented with the integral of the pitch and roll angles, that is,

$$\dot{p} = Sx, \tag{2.10}$$

where p is a $2 \times n$ matrix, $S(1,3) = 1$, $S(2,4) = 1$, and all other elements of S are zeros.

The augmented system equations then become

$$\dot{x}_s = A_s x_s + B_s u + D_s w, \tag{2.11}$$

where

$$\begin{aligned} x_s &= \left[x_p^T \;\; p^T\right], \\ A_s &= \begin{bmatrix} A_p & 0 \\ S & 0 \end{bmatrix}, \qquad B_s = \begin{bmatrix} B_p \\ 0 \end{bmatrix}, \qquad D_s = \begin{bmatrix} D_p \\ 0 \end{bmatrix}. \end{aligned} \tag{2.12}$$

3. Road Roughness Model

The input excitation to the vehicle model is assumed to be the apparent vertical roadway motion, caused by the vehicle's forward speed along a road having an irregular profile. The road surface irregularities may be treated as a stationary Gaussian random process with zero mean and characterized by a power spectral density of the form [24]

$$\mathrm{PSD}(\omega) = \frac{2\sigma^2}{\pi} \frac{\alpha v}{\omega^2 + \alpha^2 v^2}, \tag{3.1}$$

where σ^2, α, and v are the variance of road irregularities, a coefficient depending on the shape of road irregularities, and vehicle forward speed, respectively.

From the roughness representation (3.1), the vehicle excitation model can be obtained in the time domain by using a shaping filter of the form

$$\dot{z}_o = -\alpha v z_o + \xi_o, \tag{3.2}$$

where ξ_o is a zero-mean white noise process with

$$E[\xi_o(t) \cdot \xi_o(t-\tau)] = 2\alpha v \sigma^2 \delta(\tau). \tag{3.3}$$

in which $\delta(\cdot)$ denotes the Dirac delta function. The road excitation inputs to the vehicle are treated as additional states of the system. The system states are augmented with states representing the road inputs.

3.1. Uncorrelated Road Input Case

It is assumed here that the inputs at the four wheels of the vehicle are uncorrelated. In this case, the road disturbance inputs may be modeled by the following first-order differential equation:

$$\dot{w} = A_w w + I_w \xi, \tag{3.4}$$

where A_w is a 4×4 diagonal matrix with diagonal elements equal to $-\alpha v$ and I_w is a unit matrix.

Combining roadway excitation matrix (3.4) and (2.11), the results may be written as

$$\dot{x} = Ax + Bu + D\xi, \tag{3.5}$$

where

$$x = \begin{bmatrix} x_s & w \end{bmatrix}^T, \qquad A = \begin{bmatrix} A_s & D_s \\ 0 & A_w \end{bmatrix}, \qquad B = \begin{bmatrix} B_s & 0 \end{bmatrix}^T, \qquad D = \begin{bmatrix} 0 & I_w \end{bmatrix}^T. \tag{3.6}$$

3.2. Correlated Road Input Case

In this case, the correlation between the front and rear inputs on each side of the vehicle is considered. The time delay available between the front and rear input is expected to provide an opportunity to improve the rear axle actuator control. This is a sort of preview (wheelbase preview). Since all the required sensors are already available and the preview time is reasonable (L/v), where L is the wheelbase, it will be investigated here.

The pure time delay between the front and rear inputs may be represented by an Nth-order Pade approximation. The transfer function of the Nth-order Pade approximation is given in the frequency domain by

$$\frac{z_{\mathrm{lr}}(s)}{z_{\mathrm{lf}}(s)} = \frac{z_{\mathrm{rr}}(s)}{z_{\mathrm{rf}}(s)} = e^{-\tau_b s} = \frac{a_o - a_1 s + a_2 s^2}{a_o + a_1 s + a_2 s^2}, \tag{3.7}$$

where z_{lf} and z_{rf} are the front white road noise signals, z_{lr} and z_{rr} are the rear white road noise signals, and τ_b is the time delay between the front and rear inputs. For the second-order Pade approximation ($N = 2$), the constants are $a_o = 12/\tau_b^2$, $a_1 = 6/\tau_b$, and $a_2 = 1$ [25].

The state space representation of the above transfer function is given by

$$\dot{\eta}(t) = A_\eta \eta(t) + B_\eta \xi_f(t) \tag{3.8}$$

with output

$$\xi_r(t) = \xi_f(t - \tau_b) = C_\eta \eta(t) + \xi_f(t), \tag{3.9}$$

where

$$\xi_f = \begin{bmatrix} z_{\mathrm{lf}} \\ z_{\mathrm{rf}} \end{bmatrix}, \qquad \xi_r = \begin{bmatrix} z_{\mathrm{lr}} \\ z_{\mathrm{rr}} \end{bmatrix}, \qquad \eta = \begin{bmatrix} \eta_2 \\ \eta_1 \end{bmatrix}, \tag{3.10}$$

and the matrices A_η, B_η, and C_η are

$$A_\eta = \begin{bmatrix} A_{\eta 1} & 0 \\ 0 & A_{\eta 1} \end{bmatrix}, \qquad B_\eta = \begin{bmatrix} B_{\eta 1} & 0 \\ 0 & B_{\eta 1} \end{bmatrix}, \qquad C_\eta = \begin{bmatrix} C_{\eta 1} & 0 \\ 0 & C_{\eta 1} \end{bmatrix}. \tag{3.11}$$

The submatrices are

$$A_{\eta 1} = \begin{bmatrix} 0 & 1 \\ -a_o & -a_1 \end{bmatrix}, \qquad B_{\eta 1} = \begin{bmatrix} -\dfrac{12}{\tau_b} \\ \dfrac{72}{\tau_b^2} \end{bmatrix}, \qquad C_{\eta 1} = \begin{bmatrix} 1 & 0 \end{bmatrix}. \tag{3.12}$$

Equation (3.4) may be extended as

$$\dot{w} = A_w w + b_{w1} \xi_f + b_{w2} \xi_r, \tag{3.13}$$

where b_{w1}, b_{w2} are submatrices of I_w.

Substituting (3.9) into (3.13), the result may be put in the form

$$\begin{aligned} \dot{w} &= A_w w + b_{w1} \xi_f + b_{w2} C_\eta \eta + b_{w2} \xi_f \\ &= A_w w + b_{w2} C_\eta \eta + (b_{w1} + b_{w2}) \xi_f. \end{aligned} \tag{3.14}$$

It is clear from (3.14) that the rear disturbances have disappeared and hence the problem can be treated in the same way as in the uncorrelated case.

Combining (2.11), (3.8), and (3.14), the results may be written as

$$\dot{x}_f = A_f x_f + B_f u + D_f \xi_f, \tag{3.15}$$

$$\begin{aligned} x_f &= \begin{bmatrix} x_s & w & \eta \end{bmatrix}^T, \qquad A_f = \begin{bmatrix} A_s & D_s & 0 \\ 0 & A_w & b_{w2} C_\eta \\ 0 & 0 & A_\eta \end{bmatrix}, \\ B_f &= \begin{bmatrix} B_s \\ 0 \\ 0 \end{bmatrix}, \qquad D_f = \begin{bmatrix} 0 \\ b_{wf} \\ B_\eta \end{bmatrix}, \quad b_{wf} = b_{w1} + b_{w2}. \end{aligned} \tag{3.16}$$

In the case of assuming two identical front white noise signals, (3.13) may be written as

$$\dot{w} = A_w w + \left(b_{f1} + b_{f2}\right) z_{\mathrm{lf}} + \left(b_{r1} + b_{r2}\right) z_{\mathrm{lr}}, \tag{3.17}$$

where

$$b_{w1} = \begin{bmatrix} b_{f1} & b_{f2} \end{bmatrix}, \qquad b_{w2} = \begin{bmatrix} b_{r1} & b_{r2} \end{bmatrix}. \tag{3.18}$$

The problem formulation may be simplified by setting

$$\begin{aligned} &\eta = \eta_1 = \eta_2, \qquad A_\eta = A_{\eta 1}, \qquad B_{\eta 1} = B_\eta, \\ &C_\eta = C_{\eta 1}, \qquad b_{wf} = b_{f1} + b_{f2} + b_{r1} + b_{r2}. \end{aligned} \tag{3.19}$$

4. Design of Optimal Controllers

Suspension system performance criteria include ride comfort, suspension travel (working space), tire deflection (wheel load variation), static and dynamic attitude control, actuator force levels, and power consumption.

Ride comfort in a vehicle is the general feeling of well-being. It is clearly very subjective but it is generally accepted that the acceleration spectrum, particularly in the low-frequency range (1–10 Hz), is important. Root mean square (rms) value of the acceleration can be used as a measure of ride discomfort.

Suspension deflection is important from a packaging point of view; the current trends toward larger tires and lower hood designs put a premium on keeping suspension deflection as small as possible. The lateral and longitudinal forces available for cornering and/or braking depend on the normal load on the tire; clearly large dynamic variations in the normal tire force would be unacceptable. RMS values of relative displacement between the wheel and the body and of the dynamic tire deflection can be used as measures of suspension travel and wheel deflection control.

In order to obtain a control law that meets the ride comfort, ride safety (road-holding ability and body controllability), and working space (suspension travel) objectives, the following performance index is used:

$$J = E\left[\rho_1\left(\ddot{z}^2\right) + \rho_2 \sum_{j=1}^{4} \Delta_{tj}^2 + \rho_3 \sum_{j=1}^{4} \Delta_{sj}^2 + \rho_4 \sum_{j=1}^{2} p_j^2 + \rho_R \sum_{j=1}^{4} u_j^2\right], \tag{4.1}$$

where E is the expectation operator. In the performance index, ρ_1, ρ_2, ρ_3, ρ_4, ρ_R are weighting factors. The weighting factors reflect the preference of the vehicle designer. By changing the weighting factors, various control laws can be derived which place different emphases on individual aspects of performance. Δ_{sj} are suspension deflections and Δ_{tj} are tire deflections:

$$\begin{aligned} \sum_{j=1}^{4} \Delta_{tj}^2 &= (z_1 - z_{\mathrm{lf}})^2 + (z_2 - z_{\mathrm{lr}})^2 + (z_3 - z_{\mathrm{rf}})^2 + (z_4 - z_{\mathrm{rr}})^2, \\ \sum_{j=1}^{4} \Delta_{sj}^2 &= (z_1 - z_a)^2 + (z_2 - z_b)^2 + (z_3 - z_c)^2 + (z_4 - z_d)^2. \end{aligned} \tag{4.2}$$

Assume an output vector

$$y = C_f x_f \tag{4.3}$$

which contains all the important quantities to be controlled, for example, dynamic tire deflections, suspension deflections, pitch and roll motions, and so forth. C is the output matrix which may be divided into three submatrices, that is, $C_f = [C_1\ C_2\ 0]$, where C_1 is $(n_o \times n_1)$ and C_2 is $(n_o \times m)$, n_o is the number of outputs, and $n_1 = 34$.

Here, the control law for the correlated road input case is considered.

The performance index can be specified in terms of the outputs as

$$J = E\left[y^T Q y + u^T R u\right], \tag{4.4}$$

where $Q(n_o \times n_o)$ and $R(m \times m)$ are the weighting matrices. Q is a positive semidefinite matrix and R is a positive definite matrix.

The control input u that minimizes J under dynamic constraints (3.15) is given by

$$u = -R^{-1} B_f^T P_f x_f = \left[K_x \quad K_w \quad K_\eta\right] x_f = -G x_f. \tag{4.5}$$

where K_η is the additional part of the gain accounting for the time delay. The matrix P_f can be found from the solution of the algebraic Riccati equation:

$$P_f A_f + A_f^T P_f - P_f B_f R^{-1} B_f^T P_f + C_f^T Q C_f = 0. \tag{4.6}$$

The system considered here, however, is not completely controllable. This is because part of the input vector, ξ_f, in (3.15) cannot be changed by applying a control force. Consequently,

Table 1: Vehicle parameters.

Parameter	Value
Sprung mass (m_s)	1460 kg
Front unsprung mass (m_1, m_3)	40 kg
Rear unsprung mass (m_2, m_4)	35.5 kg
Spring constant of front and rear suspension spring (k_f, k_r)	18000 N/m
Tire spring constant (k_t)	175500 N/m
Sprung mass moment of inertia about longitudinal axis through sprung mass center of gravity (I_x)	460 kg·m^2
Sprung mass moment of inertia about lateral axis through sprung mass center of gravity (I_y)	2460 kg·m^2
Filter cut-off frequencies (ω_c)	3 Hz
Filter damping ratios (ζ)	0.7071
Front damping coefficient (c_f)	1088 Ns/m
Rear damping coefficient (c_r)	1030 Ns/m
Longitudinal distance from sprung mass center of gravity to front axle centerline (a)	1.00 m
Longitudinal distance from sprung mass center of gravity to rear axle centerline (b)	1.80 m
Distance between centerlines of the front tires (t_f)	1.5 m
Distance between centerlines of the rear tires (t_r)	1.5 m

the Reccati equation (4.6) can be solved numerically after separation of the unknown matrix P_f into four submatrices, as suggested by Hac [8].

The closed loop state matrix equation takes the form

$$\dot{x}_f = \left(A_f - B_f G\right)x_f + D_f \dot{\xi}_f \tag{4.7}$$

or

$$\dot{x}_f = A_c x_f + D_f \dot{\xi}_f. \tag{4.8}$$

5. Results and Discussions

The baseline data for the example vehicle model which reflects the characteristics of a typical car are given in Table 1 [18]. The improvements in vehicle ride quality through the use of optimally controlled active suspension systems are examined. The direct comparison of active and passive suspensions is difficult. While the spring and damping parameters of the conventional passive suspension remain fixed, active suspensions can be adapted to instantaneous operating conditions measured by sensors and change their characteristics to suit particular road/speed conditions or driving style. In essence, an active system can provide a soft but stable straight line ride but stiffen up for directional changes, braking, and acceleration maneuvers. To maintain fairness of comparison, the wheel-hop damping ratios for the passive system are kept the same as the ones for the active systems. It has been recognized by Elmadany [26], for both active and passive suspension systems, that the constrained placed on the damping ratio of the wheel-hop mode limits the extent to which the sprung mass acceleration can be reduced for ride comfort. However, for very lightly damped wheel-hop mode, lower road-holding qualities will result. In this study, damping ratios of 0.2 in the wheel-hop modes will be used.

Table 2: The numerical values of weighting factors.

Weighting factor	SA	SA + I
ρ_1	1.00×10^{-4}	1.00×10^{-4}
ρ_2	2.50×10^{3}	2.50×10^{3}
ρ_3	40	40
ρ_4	0	5.00×10^{3}
ρ_R	0.10	0.10

Table 3: RMS values for passive and different types of slow-active suspension systems.

Performance measure	P	SA	SA + I	SA + I, P
$\ddot{z}$ ($\times 10^{-4}$ g)	181.96	145.54	144.94	139.56
Δ_s (front) ($\times 10^{-4}$ m)	32.16	20.07	20.83	19.96
Δ_s (rear) ($\times 10^{-4}$ m)	26.62	18.17	16.34	19.63
Δ_t (front) ($\times 10^{-4}$ m)	9.98	9.58	9.58	9.57
Δ_t (rear) ($\times 10^{-4}$ m)	9.56	9.34	9.58	9.25

The following types of suspensions have been considered in the simulations

(i) Passive (P).

(ii) Slow-active with integral control terms (SA + I).

(iii) Slow-active with integral control terms and wheelbase preview (SA + I, P).

In addition, the slow-active (SA) system without integral control terms is considered where necessary to show the benefits of including the integral control terms in the design of the multivariable controllers. The numerical values of the weighting factors in the objective function used in the simulation are given Table 2. In this work, the approach used to represent the wheelbase time delay is to model it with a second-order Pade approximation. This results in a continuous control strategy to be derived for full-state feedback case. Simulations are carried out at vehicle speeds between 5 and 40 m/s, corresponding to different amount of preview. It is known that the amount of preview time depends on the vehicle speed, so as the vehicle speed increases, the preview time reduces.

5.1. Response to Random Road Disturbances

The vehicle model equipped with different suspension systems has been simulated when traveling with a constant speed of 20 m/s on a randomly profiled road. The values of the road parameters are $\alpha = 0.15$ and $\sigma^2 = 9 \times 10^{-6}\,\text{m}^2$. They correspond to a smooth (asphalt) road. In Table 3, the root mean square (rms) values of a set of selected variables are presented for the different suspensions. From Table 3, it could be noticed that the differences between the suspension systems with integral control terms and the ones without are small, due to the small weighting factors on the control terms. Therefore, only the results for systems with integral control terms are presented in the remaining portion of this section. Since the passive suspension system provides a yardstick against which other designs are evaluated, the percentage improvements in the ride quality compared with the passive system are given in Figure 8. It can be seen that the actively controlled suspensions exhibit marked improvements

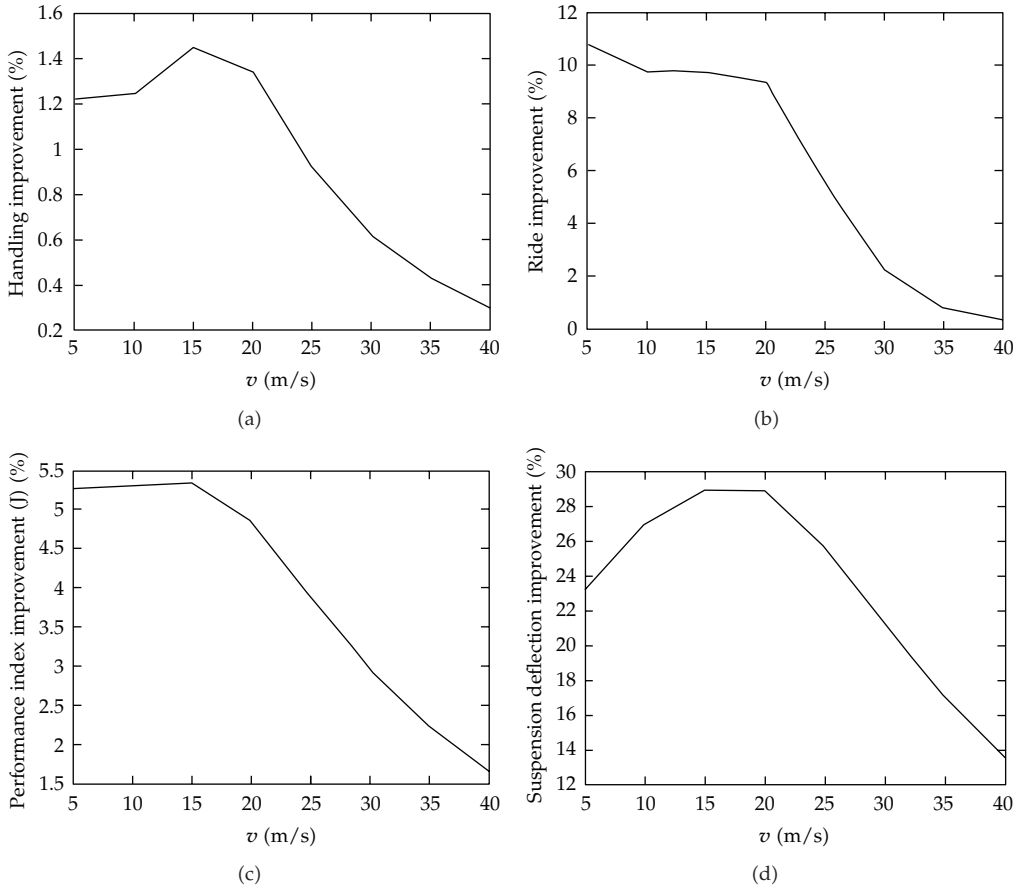

Figure 2: Percentages improvements in correlated rms values for slow-active suspension system.

in ride comfort (vibration isolation) and suspension travel without compromising the road-holding ability. In general, the results demonstrate that it is possible to improve vehicle performance by simultaneously reducing rms sprung mass acceleration and suspension deflection without negatively influencing rms tire deflections. The slow-active system gives very good performance characteristics compared to the passive system.

The improvements in the performance index, ride comfort, suspension travels (packaging), and ride handling (tire deflections), from the uncorrelated (nonpreview) case to the correlated (wheelbase preview) case, are shown in Figure 2. The improvements are particularly greater at lower vehicle speeds, as expected. For soft ride mode operation (i.e., increasing emphasis on ride comfort), more improvements in the performance capabilities are possible. The reason behind not having a greater effect on handling performance stems from the fact that the actuator has a limited bandwidth (3 Hz), and the wheel-hop resonances (around 10 Hz) are out of the range of the effective control of the actuator.

Figure 3 shows the power spectra for the vehicle running at 20 m/s. Results are given for a slow-active system with and without preview and for the passive system. The trends shown in these results are substantially the same for different vehicle speeds. The spectra show that there is very little difference between the three cases considered around wheel-hop resonances, due to the limited bandwidth nature of the system. The body acceleration

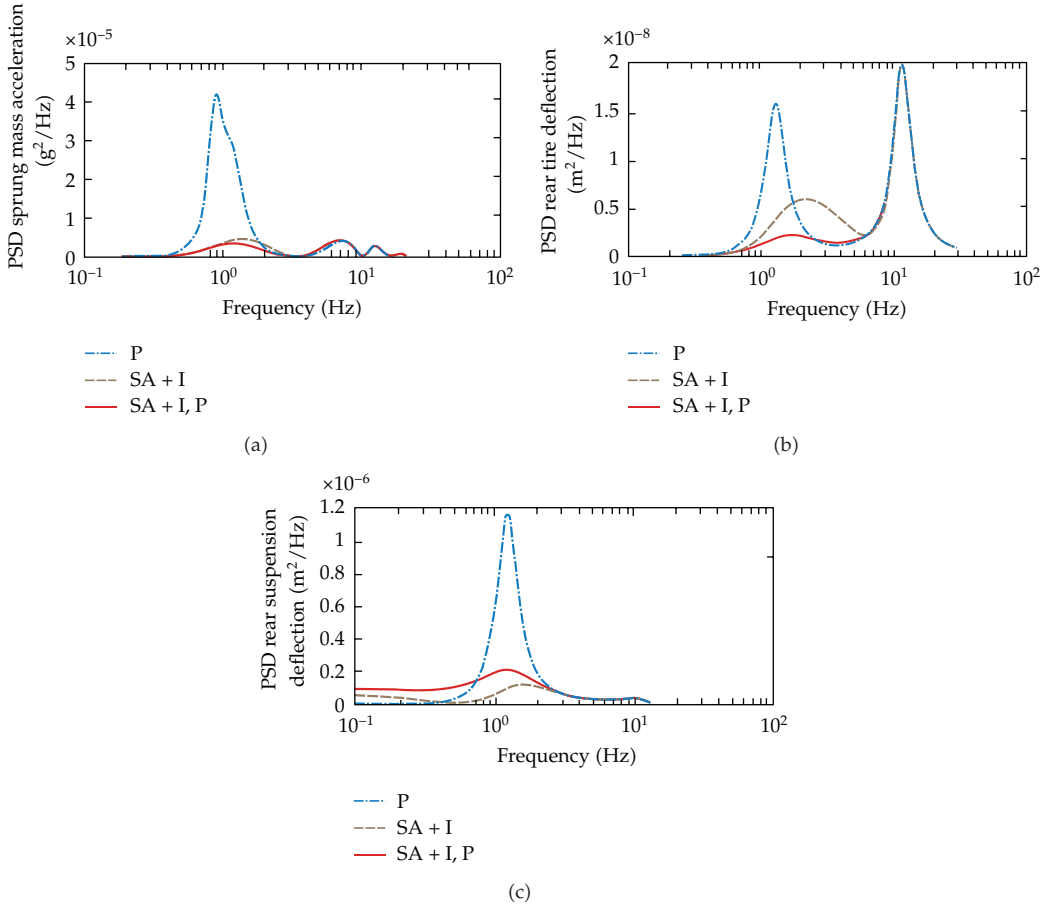

Figure 3: Response power spectra; (a) body acceleration; (b) rear tire deflection; (c) rear suspension deflection.

is improved up to 6 Hz. The rear tire deflection in the preview case is improved over the nonpreview case up to about 6 Hz. There is a marked improvement in the rear suspension deflection. At very low frequency, the preview case gives similar results as the passive system, so improving the suspension travel at low frequencies and up to wheel-hop frequency.

5.2. Response to Discrete Disturbances

Two types of discrete inputs to the vehicle system are considered. These inputs are as follows.

(1) A double bump, with the amplitude of the bumps on the right side of the car being twice as large as the bumps on the left side. This type of terrain excites both the pitch and roll modes of the sprung mass. Figure 4 presents an overhead view of the road, while Figure 5(a) presents the time histories of the bumps which the four tires experience. The vehicle speed is 20 m/s.

(2) A moment applied at the body center of gravity to simulate the vehicle behavior during accelerating. The moment increases linearly to 2000 Nm in 1 s, remains at 2000 Nm for the next 4 s, and then rolls to zero in 1 s.

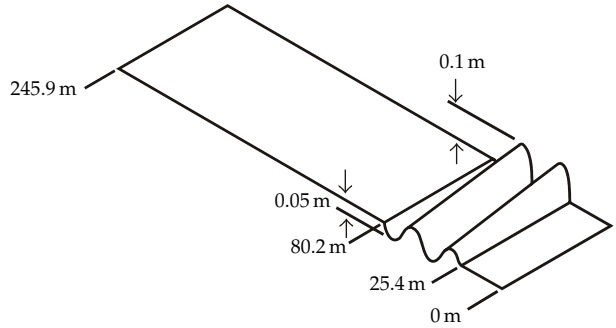

Figure 4: Double slanted bump.

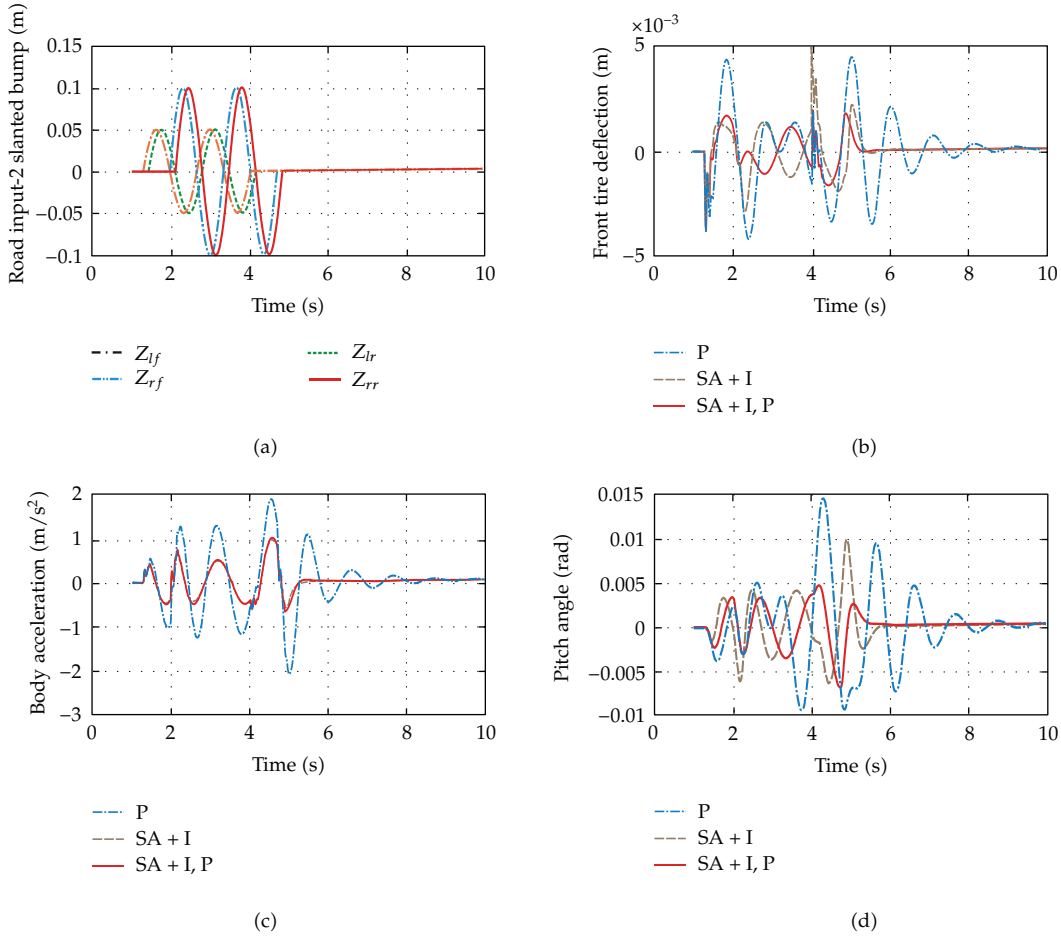

Figure 5: Response time histories; (a) road input; (b) front tire deflection; (c) body acceleration; (d) pitch angle.

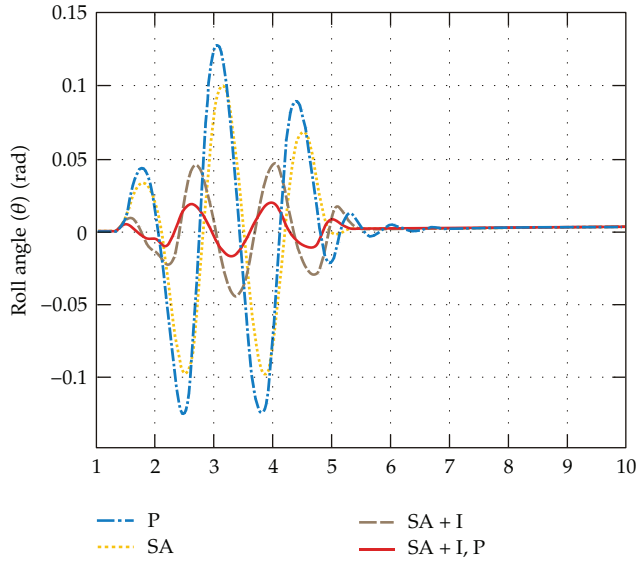

Figure 6: Pitch angle and suspension deflection responses of the actively and passively suspended vehicles to a moment applied at the sprung mass center of gravity.

The simulations are performed for the two inputs. A set of plots comparing the responses of the actively and passively suspended vehicles are presented and discussed next.

The time histories of the vehicle responses due to the double slanted bump are shown in Figures 5 and 6. From examining these figures, it may be said that the slow active suspension system exhibits smaller and better damped responses than the passive suspension. The wheel-hop damping ratio has a significant impact on the performance of the vehicle. The effect of including the integral control of the roll angle is very clear from Figure 6. The peaks of the roll angle are very much reduced compared with the ones without the integral control terms. This shows the benefit of inclusion of control terms for attitude control and ride safety.

The suspension deflection and pitch angle response time histories due to the application of a moment at the sprung mass center of gravity are shown in Figure 7. The various suspension systems have different characteristics. During accelerating the vehicle, the suspension deflection and pitch angle are not zeros for the passive system and the slow-active without the integral control of the pitch angle. These adverse effects are eliminated by introducing the integral of the pitch angle in the controller.

6. Summary and Conclusions

In this paper, linear optimal control theory has been applied to the design of the control laws for a slow-active suspension system based on a full vehicle model. The theoretical background for deriving the control laws has been reviewed for the case in which the correlation between the road inputs due to the wheelbase time delay is ignored (nonpreview). Then, the problem formulation has been modified so that the control law can account for the wheelbase preview. A second-order Pade approximation is used to represent the preview time (wheelbase time delay).

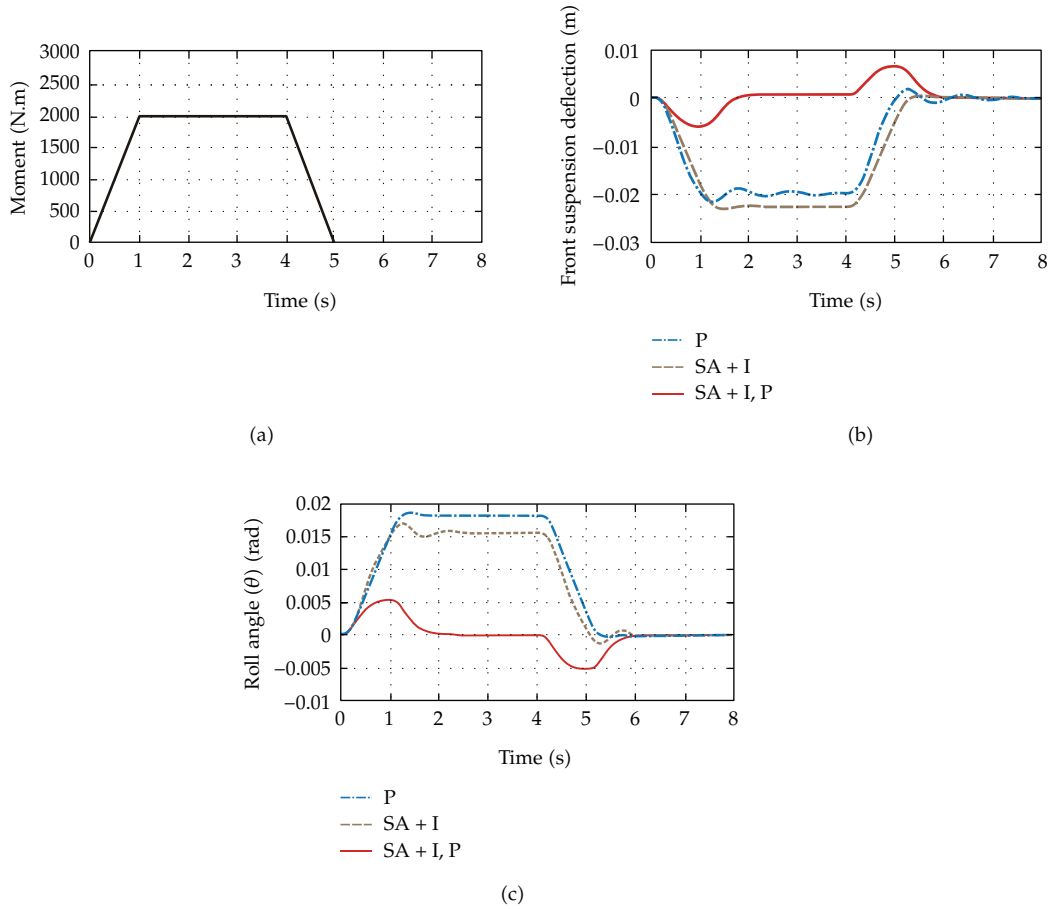

Figure 7: Percentage improvements in ride quality for all types of slow-active suspension systems comparing to passive system.

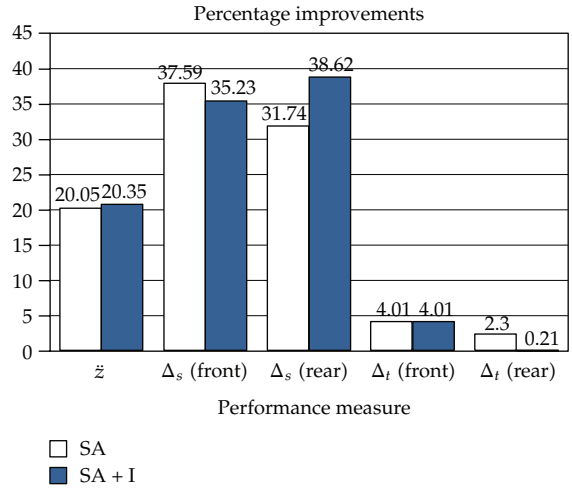

Figure 8: Percentage improvements in ride quality for all types of slow-active suspension systems comparing to passive system.

The simulation results have shown that the controller based on wheelbase preview moderately improves the general road performance of the slow-active suspensions. An improvement of about 11% at a speed of 5 m/s in ride comfort is obtained by using the wheelbase preview control strategy over than without preview. The preview control for the slow-active system makes it possible to have improvement up to 29% in the suspension working space over the nonpreview control at a vehicle speed of 20 m/s (0.14 sec preview time). The slow-active suspension system has very good performance in comparison to that of a typical passive system. It provides damping of the body resonances very effectively.

Nomenclature

A, A_s, A_p: System matrices
B, B_p, B_s: Feedback control loop input matrices
C: Output matrix
D_p, D_s: Input matrices
$\mathrm{E}(\cdot)$: Expectation operator
F_a, F_b: Total left rear and left front suspension force, respectively, (N)
F_c, F_d: Total right rear and right front suspension force, respectively, (N)
H: Transfer function matrix
I_x, I_y: Sprung mass moment of inertia about longitudinal and lateral axis through sprung mass center of gravity, respectively, (kg·m^2)
J: Performance index
K: Feedback gain matrix
P: Positive definite solution matrix of algebraic Riccati equation
Q, R, N: Weighting matrices
S: Integral matrix
T: Denotes transposition
a, b: Longitudinal distance from sprung mass center of gravity to front and rear axle center line, respectively, (m)
c_f, c_r: Damping coefficient of front and rear shock absorbers, respectively, (Ns/m)
k_f, k_r: Spring constant of front and rear suspension, respectively, (N/m)
k_t: Tire spring constant, (N/m)
m_s: Sprung mass, (kg)
m_i: Unsprung masses, $i = 1, 2, 3, 4$, (kg)
p: Integral vector
t_f, t_r: Distance between centerlines of the front and rear tires, respectively, (m)
u: Control input vector
u_i: Actuator control demand signal, $i = 1, 2, 3, 4$
u_i': Second-order filtered control demand signal, $i = 1, 2, 3, 4$
u_i'': Fourth-order filtered control demand signal, $i = 1, 2, 3, 4$,
v: Forward vehicle speed, (m/s)
w: Vector of road inputs
x: Input signal
x_p, x_s: State vectors
y: Output signal
z: Vertical position of sprung mass center of gravity, (m)
z_a, z_b: Vertical position of left front and left rear corners of sprung mass, respectively, (m)

z_c, z_d: Vertical position of right front and right rear corners of sprung mass, respectively, (m)
$z_{\mathrm{lf}}, z_{\mathrm{lr}}$: Height of road under left front and left rear unsprung mass, respectively, (m)
$z_{\mathrm{rf}}, z_{\mathrm{rr}}$: Height of road under right front and right rear unsprung mass, respectively, (m)
z_1, z_2: Vertical position of left front and left rear unsprung mass, respectively, (m)
z_3, z_4: Vertical position of right front and right rear unsprung mass, respectively, (m)
z_5, z_6: Displacement of left front and left rear slow active actuator, respectively, (m)
z_7, z_8: Displacement of the right front and right rear slow active actuator, respectively, (m)
Δ_{sj}: Suspension deflection, $j = 1, 2, 3, 4$, (m)
Δ_{tj}: Tire deflection, $j = 1, 2, 3, 4$, (m)
α: A coefficient depending on the shape of road irregularities, (m^{-1})
$\delta(\cdot)$: Dirac delta function
ζ: Damping ratio
ξ_o: Zero mean white noise process
ρ_i: Weighting factors $i = 1, 2, 3, 4$
ρ_R: Control weighting factor
σ^2: Variance of road irregularities, (m^2)
τ: The time constant (s)
ϕ, θ: Roll and pitch angles of sprung mass, respectively, (rad)
ω: Circular frequency, (rad/s)
ω_c: Filter cut-off frequency, (Hz).

Acknowledgment

The author would like to thank the College of Engineering Research Center—Deanship of Scientific Research at King Saud University—for funding and supporting this research.

References

[1] J. P. C. Gonçalves and J. A. C. Ambrósio, "Road vehicle modeling requirements for optimization of ride and handling," *Multibody System Dynamics*, vol. 13, no. 1, pp. 2–23, 2005.

[2] J. Lu and M. DePoyster, "Multiobjective optimal suspension control to achieve integrated ride and handling performance," *IEEE Transactions on Control Systems Technology*, vol. 10, no. 6, pp. 807–821, 2002.

[3] M. A. Karkoub and M. Zribi, "Active/semi-active suspension control using magnetorheological actuators," *International Journal of Systems Science*, vol. 37, no. 1, pp. 35–44, 2006.

[4] G. N. Jazar, R. Alkhatib, and M. F. Golnaraghi, "Root mean square optimization criterion for vibration behaviour of linear quarter car using analytical methods," *Vehicle System Dynamics*, vol. 44, no. 6, pp. 477–512, 2006.

[5] M. O. Abdalla, N. Al Shabatat, and M. Al Qaisi, "Linear matrix inequality based control of vehicle active suspension system," *Vehicle System Dynamics*, vol. 47, no. 1, pp. 121–134, 2009.

[6] K. Hyniova, A. Stribrsky, J. Honcu, and A. Kruczek, "Active suspension system with linear electric motor," *WSEAS Transactions on Systems*, vol. 8, no. 2, pp. 278–287, 2009.

[7] A. Akbari and M. Geravand, "Output feedback constrained H^∞ control of active vehicle suspensions," in *Proceedings of the 2nd IEEE International Conference on Advanced Computer Control (ICACC '10)*, vol. 3, pp. 399–404, Shenyang, China, March 2010.

[8] A. Hac, "Suspension optimization of a 2-dof vehicle model using a stochastic optimal control technique," *Journal of Sound and Vibration*, vol. 1, no. 3, pp. 343–357, 1985.

[9] R. M. Chalasani, "Ride performance potential of active suspension systems-part I: simplified analysis based on quarter car model," in *Proceedings of the Symposium on Simulation and Control of Ground Vehicles and Transportation Systems, ASME Winter Annual Meeting*, vol. 80, pp. 187–204, ASME, Anaheim, Calif, USA, December 1986.

[10] M. B. Goran, B. I. Bachrach, and R. E. Smith, "The design and development of a broad bandwidth active suspension concept car," in *Proceedings of the 24th FISITA Congress on Total Vehicle Dynamics (IMechE Paper 925100)*, vol. 2, pp. 231–252, 1992.

[11] M. M. Elmadany and Z. S. Abduljabbar, "Linear quadratic Gaussian control of a quarter-car suspension," *Vehicle System Dynamics*, vol. 32, no. 6, pp. 479–497, 1999.

[12] M. M. Elmadany and M. I. Al-Majed, "Quadratic synthesis of active controls for a quarter-car model," *Journal of Vibration and Control*, vol. 7, no. 8, pp. 1237–1252, 2001.

[13] P. Gaspar, I. Szaszi, and J. Bokor, "Design of robust controllers for active vehicle suspension using the mixed μ synthesis," *Vehicle System Dynamics*, vol. 40, no. 4, pp. 193–228, 2003.

[14] D. A. Mantaras and P. Luque, "Ride comfort performance of different active suspension systems," *International Journal of Vehicle Design*, vol. 40, no. 1–3, pp. 106–125, 2006.

[15] R. S. Sharp and S. A. Hassan, "On the performance capabilities of active automobile suspension systems of limited bandwidth," *Vehicle System Dynamics*, vol. 16, no. 4, pp. 213–225, 1987.

[16] S. M. El-Demerdash and D. A. Crolla, "Effect of non-linear components on the performance of a hydro-pneumatic slow-active suspension system," *Proceedings of the Institution of Mechanical Engineers*, vol. 210, no. 1, pp. 23–33, 1996.

[17] Y. Aoyama, K. Kawabata, S. Hasegawa, Y. Kobari, M. Sato, and Tsuruta, "Development of the full active suspension by Nissan," Society of Automotive Engineers 901747, 1990.

[18] Y. Yokoya, K. Ryotiei, H. Kawaguchi, K. Ohashi, and H. Otino, "Integrated control system between active control suspension and four-wheel steering for the 1989 Celica," Society of Automotive Engineers 901748, 1990.

[19] A. Hac, "Optimal linear preview control of active vehicle suspension," *Vehicle System Dynamics*, vol. 21, no. 3, pp. 167–195, 1992.

[20] M. M. Elmadany, Z. Abduljabbar, and M. Foda, "Optimal preview control of active suspensions with integral constraint," *Journal of Vibration and Control*, vol. 9, no. 12, pp. 1377–1400, 2003.

[21] N. Louam, D. A. Wilson, and R. S. Sharp, "Optimal control of vehicle suspension incorporating the time delay between front and rear inputs," *Vehicle System Dynamics*, vol. 17, no. 6, pp. 317–336, 1988.

[22] R. S. Sharp and D. A. Wilson, "On control laws for vehicle suspensions accounting for input correlations," *Vehicle System Dynamics*, vol. 19, no. 6, pp. 353–363, 1990.

[23] A. Pilbeam and R. S. Sharp, "On the preview control of limited bandwidth vehicle suspensions," *Proceedings of the Institution of Mechanical Engineers*, vol. 207, no. 3, pp. 185–193, 1993.

[24] R. W. Rotenberg, *Vehicle Suspension*, Mašinostrojenie, Moskou, Russia, 1972.

[25] M. Athans and P. L. Falb, *Optimal Control*, McGraw-Hill, New York, NY, USA, 1966.

[26] M. M. Elmadany, "Optimal linear active suspensions with multivariable integral control," *Vehicle System Dynamics*, vol. 19, no. 6, pp. 313–329, 1990.